

Disease-economy trade-offs under alternative epidemic control strategies

Thomas Ash, Antonio M. Bento*, Daniel Kaffine, Akhil Rao, Ana I. Bento*

Abstract

Public policy and academic debates regarding pandemic control strategies note disease-economy trade-offs, often prioritizing one outcome over the other. Using a calibrated, coupled epi-economic model of individual behavior embedded within the broader economy during a novel epidemic, we show that targeted isolation strategies can avert up to 91% of economic losses relative to voluntary isolation strategies. Unlike widely-used blanket lockdowns, economic savings of targeted isolation do not impose additional disease burdens, avoiding disease-economy trade-offs. Targeted isolation achieves this by addressing the fundamental coordination failure between infectious and susceptible individuals that drives the recession. Importantly, we show testing and compliance frictions can erode some of the gains from targeted isolation, but improving test quality unlocks the majority of the benefits of targeted isolation.

*Corresponding author: abento@usc.edu or abento@iu.edu

We thank Jude Bayham, Matthew G. Burgess, Dana Goldman, Adam Rose and Matthew Ferrari for helpful comments.

To date, over 190 million individuals have been infected with SARS-CoV-2 and more than 4 million have died worldwide, with around fifteen percent of these deaths happening in the United States, and only around 26% of the world's population has received at least one vaccination [1]. The pandemic also triggered the sharpest economic recession in modern American history. According to the Commerce Department, during the second quarter of 2020 US Gross Domestic Product shrank at an annual rate of 32.9 percent [2]. The COVID-19 pandemic's global repercussions exposed a need for coupled-systems frameworks that link epidemiological and economic models and assess potential disease-economy trade-offs. Such frameworks can reveal important features of control strategies, such as the role of targeted isolation strategies that can overcome the fundamental coordination failure between infectious and susceptible individuals that drives the economic recession.

Broadly, four areas of study have informed the assessment of control strategies. Epidemiological studies evaluate disease dynamics and consider the heterogeneity of impacts resulting from control strategies [3, 4, 5, 6, 7, 8, 9, 10, 11, 12]. Epi-economics studies consider the micro-foundations of human behavior as drivers of the disease, as well as the costs and benefits of alternative control strategies [13, 14, 15, 16, 17, 18, 19, 20, 21, 22, 23]. An emerging literature on the macroeconomic consequences of pandemics considers the impacts of COVID-19 and various control strategies, either by embedding these behaviors in a broader economy with disease dynamics [24, 25] or by conducting detailed macroeconomic projections in the absence of disease dynamics [26, 27]. In addition, numerous statistical analyses have examined the relationship between disease-related behaviors and economic activity [28, 29, 30]. Several knowledge gaps remain. For example, structurally mapping economic activities to contacts in a tractable fashion that retains the underlying heterogeneity of the population presents various challenges. One major challenge is how to calibrate this mapping using epidemiological social contact surveys, which contain data on potentially disease-transmitting contacts between individuals. Further, detailed individual economic behavior and epidemiological transmission mechanisms have typically not been embedded into models that consider the broader economy. Finally, the set of control strategies considered in coupled-systems models remains limited and overly-simplified. To date, these models have not included individual-focused targeted isolation strategies, and the conditions under which they may overcome disease-economy trade-offs are unknown.

To address these gaps, we develop a tractable coupled epi-economic model of microeconomic behavior embedded within the broader economy. Fig.1 presents a schematic representation of our model. Dynamic, forward-looking consumption and labor-leisure choices that account for the risk of infection are made by either A) decentralized individuals or B) coordinated policy interventions. These choices generate contacts which evolve endogenously in the model—i.e., contact rates affect and are affected by the disease dynamics. Depending on the activity, contacts can be avoidable or unavoidable. For example, in the U.S. economy, the average individual has around 7.5 contacts at their place of work during an 8-hour workday. These are avoidable contacts if the individual can alter their labor supply. In contrast, contacts such as those that occur at home are unavoidable and carry a risk of infection [31]. For analytical tractability, the framework initially assumes individuals have full information about their health status, and the presence of pre-symptomatic and asymptomatic individuals is reflected in the calibration of productivity losses as only individuals with no or mild symptoms will be able to work. The model solves the dynamic optimization problem of balancing risk and activity and aggregates the solution across the population, permitting direct calculation of disease-economy trade-offs. Solutions to these types of dynamic optimization problems describe forward-looking individual behavior [32]. Forward-looking behavior is critical to modeling expectations during the pandemic, but imposes a steep computational costs as the dimension of the state space increases [33], necessitating our modelling assumptions for elements not central to our analysis.

In a decentralized choice setting, infectious individuals put susceptible individuals at risk and bear no direct consequences for this imposition (in economics terminology, an infectious individual creates a *negative externality* on a susceptible individual). Thus, a key challenge for disease control and avoiding economic losses is the inability of susceptible individuals to coordinate with infectious individuals and encourage them to reduce their activities and contacts [34]. Absent such coordination, susceptible

individuals bear the full burden of adjusting their consumption and labor choices to minimize personal risk - we refer to this decentralized control strategy as “voluntary isolation.” Recognizing this coordination failure, we consider a policy intervention whereby a central planner optimally coordinates labor and consumption choices, yielding a control strategy that targets infectious individuals—“targeted isolation.” In a world where the coordination failure is resolved, e.g., by paying infectious individuals to isolate, susceptible individuals can still consume, work, and engage in contacts, minimizing individual economic losses and the resulting recession. Importantly, to illustrate the general benefits of such targeting strategies, we abstract from many aspects of individual heterogeneity, often captured in epidemiological studies (e.g., [35, 36, 9, 37]). This is reasonable, since the fundamental coordination failure is itself independent of heterogeneity (see SI).

In real-world terms, a targeted isolation policy encompasses any interventions aimed at encouraging infectious individuals to isolate themselves, with susceptible individuals isolating only if necessary to suppress infection growth. Such a policy would contain features like incentive payments to encourage individuals to obtain tests following possible exposure or symptoms, incentive payments for individuals to isolate following positive tests (e.g., compensation for lost wages), randomized compliance checks and penalties for individuals caught breaking isolation, etc. Implementation of such targeted isolation policies may be imperfect; we examine compliance scenarios to assess the degree to which such issues may limit the performance of targeted isolation policies.

We calibrate our model to pre-pandemic economic and social mixing data, using 2017 contact survey data from [6] and next-generation matrix methods [38] to generate a contact function linking different economic activities to contacts and to calibrate the transmission rate (see SI). Alternative parameter choices consider the role of online shopping and work that may have altered the underlying relationships between activities and contacts (see SI). The results described below hold across a wide range of plausible economic and epidemiological parameters.

We study the disease-economy trade-offs that result from three alternative control strategies: voluntary isolation, targeted isolation, and a blanket lockdown (see Materials and Methods). Under voluntary isolation, decentralized individuals continue to optimize their personal behavior based on preferences and health status. Some may isolate, others will not. By contrast, a policy of targeted isolation of infectious individuals is able to address the coordination failure, effectively separating susceptible individuals from infectious ones. Finally, to contrast these results against a commonly used control strategy, we also consider a blanket lockdown, whereby all individuals are forced to isolate, independent of their disease status. In the U.S., for example, by April 15 2020, more than 95% of the population was under a stay-at-home order [29, 39]; such social distancing policies have been noted for their large economic costs and social disruption. Our focus is on the behavioral channels each policy utilizes to deliver disease control and economic benefits rather than the timing of policy implementation.

Our first contribution is the development of the tractable coupled epi-economic model described above that highlights the mechanisms and benefits that targeted isolation strategies have the potential to deliver. As noted, this model must prioritize the key mechanisms (e.g. the link between contacts and economy; the coordination problem) and impose valid assumptions to remain tractable in the face of steep computational costs. Of course in practice, implementing such targeted isolation strategies comes with challenges, particularly as our key assumption of full information regarding disease status may not hold in the early stages of an emerging disease epidemic. Thus, our second contribution is to apply the above model to consider a number of important frictions in a tractable way—for example, we allow for initial tests to be slow and of low specificity and sensitivity, which then improve over the course of the pandemic. This application demonstrates how our modeling approach can be applied to address some of the challenges associated with integrated disease models identified in [40].

We show that the widely-used control strategies of voluntary isolation or blanket lockdowns suppress the epidemic nearly as effectively as targeted isolation, but are economically costly and impose a much deeper recession. Targeted isolation strategies avoid these sharp disease-economy trade-offs by incen-

tivizing infectious individuals to isolate. This allows susceptible individuals to continue to consume and work, carrying the economy through the epidemic with a milder recession. Using targeted isolation strategies instead of voluntary isolation strategies can avert substantial costs—up to the order of \$3.5 trillion in averted recessionary losses. Importantly, we show that relevant frictions (testing information, compliance) can erode some of the gains from targeted isolation, but availability of high-quality tests unlocks the majority of the benefits of targeted isolation. An implication of these findings is that the relative merits of targeted isolation versus blanket lockdowns at any given point in time depend on the test environment and other features of the emerging disease system.

In the following sections, we begin by abstracting from information- and compliance-related frictions in order to illustrate the key model mechanisms and our methodological contributions. That is, we assume all agents perfectly know their health status and the current distribution of health statuses across the population, and fully comply with all policy mandates. Having established the underlying mechanisms, we then analyze a model application that introduces lags in test reporting, uncertainty due to limited test quality, and partial compliance with lockdown strategies and targeted isolation.

Results

Methodological contributions

Our first contribution is methodological: we construct a data-driven, theoretically-consistent coupled epi-economic model which can be used to study important properties of novel pathogens in economies. We emphasize two core model features. First, regardless of control strategy, in our model the SARS-CoV-2 epidemic spreads rapidly in the population, with peak daily incidence early in the epidemic (Fig. 2A & C), and final proportions of the population exposed (Fig. 2C) and fatalities (Fig. S2) are largely unaltered. A plausible blanket lockdown designed to minimize total cases (see SI 4.1) can indeed reduce cases relative to targeted or voluntary isolation strategies, however it leads to a rebound (Fig. 2A) when the lockdown is relaxed (observed in all blanket lockdown scenarios considered—Fig. S4 & Fig. S7). Second, under a targeted isolation strategy, disease control does not come at as large an economic cost as under voluntary isolation or a case-minimizing blanket lockdown (Fig. 2B & C). In aggregate terms, targeted isolation converts an historically-severe recession (66% peak-to-trough contraction under voluntary isolation, 84% under the blanket lockdown) to a mild and not-atypical one (3% peak-to-trough contraction). By coordinating individuals’ behavior over the course of the epidemic, targeted isolation can minimize the disease-economy trade-off imposed by voluntary isolation and blanket lockdown strategies.

The large economic savings (91% of individual economic losses averted) and the marked difference in the probability of contact (Fig. 3B) from the targeted isolation strategy arise primarily from shifting the burden of isolating from susceptible to infectious individuals (Fig. 3A). Under a voluntary isolation strategy, some infectious individuals continue to work and consume despite the risk they impose on others [41, 42, 43]. This is the key coordination failure that increases the probability of infection (Fig. 3B) and forces susceptible individuals to work and consume less to avoid infection (Fig. 3A). Since susceptible individuals are the majority of the population in a novel epidemic, this approach to disease control comes at a large economic cost. By contrast, targeting isolation at infectious individuals dramatically changes the composition of the pool of people working and consuming (Fig. 3A & B). Voluntary isolation at the epidemic peak leads to about 3 fewer hours spent at consumption activities and 6 fewer hours spent at labor activities per day by *susceptible* individuals, while targeted isolation reduces *infectious* individuals’ activities by similar amounts (Table S2). This does not cause changes in mean daily contacts between strategies (Fig. 3C & D), nor prevalence by activity type (Fig. 3E), even though many more susceptible individuals are able to work and consume. As a consequence, targeting delivers small improvements in infection outcomes but massive economic savings.

Model applications

Our second contribution is to apply the model to COVID-19 in the US and study how key frictions with plausible magnitudes may affect the model mechanisms and resulting policy conclusions. We focus on two types of frictions which are particularly relevant to novel epidemics: limited or delayed health status information, and individual non-compliance with policy directives. These frictions are modeled as particular scenarios (see Materials and Methods). Importantly, we deliver a tractable and plausible analysis of these frictions in a coupled epi-economic model, though we acknowledge that there is much research to be done on the microeconomic foundations of individual behavior in the face of a novel pathogen.

Our first scenarios vary test quality and the time between taking a test and receiving results (Figure 4). In the “limited and delayed testing” scenario (10% test quality, 8 day test lag), targeted isolation can only recover around 13% of the economic benefits from targeted isolation in the baseline scenario, and only around 30% of the infection control benefits from targeting. In the “improving test quality” scenario (95% test quality after 75 days, 8 day test lag), targeted isolation can recover nearly 92% of the economic benefits from targeting in the baseline scenario, and nearly 94% of the infection control benefits. These results are largely unchanged in the “improving test quality and delays” scenario (95% test quality after 75 days, 5 day test lag after 60 days). The improvement in test timeliness has very little effect over and above the effect of improved test quality, and the changes in transient dynamics can even reduce some of the economic and infection control benefits. In all cases, the voluntary or targeted isolation policies deliver substantial economic benefits over blanket lockdowns, while blanket lockdowns deliver greater infection control benefits. We explore the robustness of these results to alternative assumptions on equilibrium behavior under low-quality information, finding it does not change the ranking of policies in terms of economic benefits but may alter the ranking over infection control benefits (see SI 3.3.4).

These results highlight two important channels through which targeted isolation delivers improvements over voluntary isolation. First, as expected, better information tends to enable better implementation of targeted isolation. Second, however, better information can also worsen the recession under voluntary isolation. Intuitively, poor information mitigates the coordination failure by leading individuals uncertain about their health type to act as though they are a different type. Many infectious individuals who would otherwise impose externalities on others end up acting as though they are susceptible and reducing their labor supply and consumption. Similarly, many susceptible individuals act as though they are asymptomatic or recovered and continue to supply labor and consume, mitigating the recession severity.

Our next scenarios vary the fraction of individuals who comply with policy mandates such as blanket lockdowns or targeted isolation (Figure 5). In the “low compliance and perfect information” scenario (0% compliance rate, no information frictions), targeted isolation is ineffective. In the “partial compliance and perfect information” scenario (75% compliance, no information frictions), targeted isolation recovers just over 76% of the economic benefits from targeting in the baseline scenario, and nearly all of the infection control benefits. These results are intuitive given the properties of targeted and voluntary isolation in the baseline model: since the non-compliant share of the population behaves as they would under voluntary isolation, the benefits realized are a convex combination of those from voluntary and targeted isolation. Finally, in the “partial compliance and improving information scenario” (75% compliance, 95% test quality after 75 days, 5 day test lag after 60 days), targeted isolation recovers roughly 95% of the economic benefits from targeting in the baseline scenario, and roughly 95% of the infection control benefits as well. Although compliance is unchanged, the percentage of benefits obtained improve for the same reason as in the purely information scenarios – worse information at certain levels can improve outcomes as infectious individuals act as susceptibles solving the coordination failure (see previous paragraph). Taken together, our results provide qualitative insights into the importance of information quality, information timeliness, and compliance on the benefits of targeted isolation policies.

Robustness to assumptions on coupling parameters and functions

To assess the robustness of our conclusions to these modeling choices, we conduct some sensitivity analysis over the relevant model parameters. We calibrate the contact function using pre-pandemic contact data, and to keep the model tractable we incorporate the impact of asymptomatic individuals through productivity losses as well as use a functional form for the contact function that implies individuals have identical contact levels. We focus on the core model, devoid of information- or compliance-related frictions, to identify how these modeling choices affect the maximum possible gains from targeted isolation.

First, we show the mapping between prevalence of asymptomatic individuals and productivity losses from infection in Fig.6A. Higher prevalence of asymptomatic individuals in the population imply lower productivity losses incurred by a representative infectious agent. Second, because structural changes in the economy during the pandemic may have reduced the number of contacts per unit of activity (e.g., increased prevalence of contactless goods delivery), we examine our findings' robustness by altering the ratios of contacts at different activities and changing the functional form of the contact function. Fig.6B-E show how our conclusions about targeted isolation relative to voluntary isolation change as we vary the contact structure of the economy and the proportion of non-severely-diseased individuals. From the white dots (main model calibration), moving to the left in Fig.6B-E shows that lower prevalence of asymptomatic individuals will increase the economic effectiveness of targeted isolation without affecting the relative number of cases averted. Moving up the vertical axis in Figs.6B-C shows that increasing the share of contacts which occur at consumption rather than labor activities (e.g., if remote work becomes more common while bars and restaurants remain open) would again increase the economic effectiveness of targeted isolation without affecting the relative number of cases averted. Moving up the vertical axis of Fig.6D-E shows that increasing the share of contacts at unavoidable activities (e.g., if consumption and labor become increasingly contactless) will reduce the economic effectiveness of targeted isolation without affecting the relative number of cases averted. The functional form of the contact function allows us to examine heterogeneity in contact rates—Fig.6F-G. Convex contact functions emerge when high-contact activities (individuals) are reduced (isolated) first and concave functions emerge when high-contact activities (individuals) are reduced (isolated) last. Targeted isolation accounting for these choices is likely to produce convex contact functions if high-contact activities (individuals) are reduced (isolated) first. We find such variations have a modest impact on the economic effectiveness of targeted isolation, but do not affect its disease control properties. We discuss these forms further in Materials and Methods and the SI and show the sensitivity of our findings to plausible variations in other structural parameters in SI Figure S6.

Discussion

More than a year into the SARS-CoV-2 pandemic, it is increasingly clear economic concerns cannot be neglected [44]. We show that even in scenarios with imperfect testing and compliance, a targeted isolation approach emerges from our model as an optimal strategy which balances disease spread and economic activities. Our predicted infection rates and economic responses are broadly consistent with observed patterns (see SI 2.7), and thus our results likely capture the correct order of magnitude and capture the key qualitative features of the epidemic and recession.

Recent studies suggest the COVID-19 recession was driven by voluntary reductions in consumption in response to increasing infection risk [28, 45]. We show this drop in consumption is driven by a coordination failure: infectious individuals do not face the full social costs of their activities, leading susceptible individuals to withdraw from economic activity. This coordination failure resembles the classical problem of the tragedy of the commons in natural resources and the environment [46, 47, 48], underscoring the lack of property rights in the market for infection-free common spaces. It also shares similarities with coordination issues that emerge in climate change, fisheries, orbit use and other settings [49, 50, 51, 52]. Correcting this coordination failure via a targeted isolation strategy that internalizes the costs infectious

individuals impose on susceptible individuals delivers substantial economic savings (Fig.2 & Fig.3).

Our conclusions arise from a data-driven method to calibrate the mapping between disease-transmitting contacts and economic activities. Compartmental models of infectious diseases typically segment activities based on population characteristics like age and student status (e.g., [35, 36, 7, 53, 54]) rather than economic choices like consumption and labor. We build on prior work in this area (e.g. [15, 16, 18]) to address two long-standing challenges: appropriately converting units of disease-transmitting contacts into units of economic activities (contacts into dollars and hours), and calibrating the resulting contact function to produce the desired \mathcal{R}_0 . We address these challenges in three steps (see Materials and Methods and SI).

First, we use contact matrices from [6] to construct age-structured contact matrices at consumption, labor, and unavoidable other activities (Fig. S1). We then use next-generation matrix methods to calculate the mean number of contacts, adjusted for how individuals of different ages mix with each other, at each activity. Finally, we use these values with pre-epidemic consumption and labor supply levels to map contacts to dollars and hours in the contact function, and then calibrate the \mathcal{R}_0 . This approach provides a behaviorally-grounded perspective on why contacts occur. Understanding the structure and benefits of targeted isolation requires this mapping between economic activities and contacts.

Our results also serve to highlight an important benefit of making high-quality testing for novel pathogens widely available early on [55, 56, 57, 58]—it facilitates targeted isolation approaches which reduce economic losses. Targeted isolation provides the greatest benefits when information quality and compliance are high, with testing lags playing a relatively minor role. These results suggest that by enabling targeted isolation policies, early provision of high-quality testing combined with incentives to comply with policy directives can unlock some infection control benefits and substantial economic benefits. When testing is low-quality throughout the epidemic, the targeted isolation solution resembles a blanket lockdown (see Fig. 4).

While we have shown that information frictions and non-compliance can be important factors limiting policy effectiveness, we stress the fundamental problem is an inability to coordinate among susceptible individuals. In an ideal world, a market would exist allowing susceptible individuals, who do not want to be exposed to infection, to club together to pay infectious individuals to stay out of common spaces (e.g., gyms, restaurants, supermarkets). Even in the face of information and compliance issues, this would solve the fundamental problem and allow susceptible individuals to continue working and consuming, removing the disease-economy trade-off inherent in lockdown approaches. In reality this is not possible, since susceptible individuals cannot coordinate (from economic theory, no “property rights” exist determining specifically whether susceptible or infectious individuals have a right to enter these spaces, and thus dictating who should be paid for access to them as is true in most markets) [59]. Since this ideal or first best solution is not possible, targeted isolation is a policy solution to solve this coordination problem.

To implement targeted isolation, governments can provide incentives and encouragement for infectious individuals to remove themselves from these public spaces. In our model, paying individuals to stay home while infectious would require spending on the order of \$428 billion (two weeks pay times the total number of infected), to purchase the gain of an avoided recession on the order of \$4 trillion—total savings of up to \$3.5 trillion relative to voluntary isolation (see Fig. 2), not including additional averted costs from long-term negative public health outcomes [27]. Our focus here is on the benefits of targeted isolation strategies rather than the details of how to implement them, or on cross-regional comparisons of implemented strategies (see SI 5.4.1 for more discussion); designing such incentive mechanisms presents its own challenges, e.g., [60, 14, 10], and is an important area for future research. However, through our compliance scenarios we also demonstrate the effect of improperly implemented targeted isolation.

Given the appealing features of targeted isolation strategies, is there still a role for blanket lockdowns? On the one hand, blanket lockdown strategies can reduce burdens on hospital systems, particularly in the initial phase, [53, 61], while on the other hand, the rebound effects may still induce substantial strains on

hospital systems later on (Fig. S6). The excessive costs and rebound effects are robust features of blanket lockdowns, both in our model (Fig.S4 & Fig. S7) and confirmed in previous studies, e.g., [62, 63, 11]. The rebound size in our model is also large—nearly 100% of cases averted during the blanket lockdown reoccur later on. While “targeted lockdowns” that lock down areas or businesses burdened with higher transmission rates [64, 65] avoid some of the excess costs of blanket lockdowns, they are still blunt instruments compared to targeted isolation. Nonetheless, blanket lockdowns and targeted isolation strategies may be complementary—blanket lockdowns reduce hospitalization burdens in the early days when test quality is low, and targeted isolation manages rebound effects by correcting the coordination problem once test quality has increased. Our analysis suggests the optimal time to switch from blanket lockdowns to targeted isolation will depend critically on test quality. Finally, while ensuring compliance with targeted isolation may be more costly than ensuring compliance with blanket lockdowns, we show that for many plausible lockdown designs the targeted isolation compliance costs would have to be very large to overturn the cost savings from targeted isolation (see Figure 7 row 2 and Figure 2—roughly \$17,000 per person—or see SI Figure S5).

As vaccines are being deployed, new SARS-CoV-2 variants are now circulating in many countries [66]. Thus it continues to be critical to avoid premature relaxation of disease-economy management measures [30]. Our results carry insights for vaccine deployment, to the extent vaccination limits infectiousness. Since our model shows that one infectious individual failing to isolate will induce many susceptible individuals to withdraw, our model insights are consistent with prioritizing vaccines to individuals who, when infectious, are least likely or able to isolate (and therefore most likely to contribute to spread). Using targeted isolation throughout vaccine delivery can further reduce economic costs and disease burden.

There remain many opportunities and open challenges in coupled-systems modelling of disease control and economy management. There is important heterogeneity in transmission, infectiousness, and exposure (e.g., superspreading events and crowding [67, 68]), though explicitly incorporating such heterogeneity into the coupled systems is non-trivial. Our model applications have demonstrated one way to tractably introduce such features into a rational epidemic setting. As greater amounts of high-fidelity mobility data become available, it is important to build data-driven mappings between mobility, contacts, and economic activities within transmission models—[69, 70, 10, 71] offer promising steps in this direction. However, connecting mobility to contact rates and infection probabilities (given a contact) will require further consideration. Finally, it is critically important to consider how to design incentives and measure the costs of implementing targeted isolation programs which can sustain participation and compliance.

As an endgame strategy, targeted isolation could avert trillions in recessionary losses while effectively controlling the epidemic. Put differently, disease-economy trade-offs are inevitable when the coordination failure cannot be resolved. Amidst the ongoing public policy debate about economic relief, lockdown fatigue, and epidemic control [26], allocating funds to solving the coordination problem—providing incentives for infectious individuals to learn their disease status and isolate—likely passes the cost-benefit test.

Methods

Here we provide an overview of the key elements of our framework including describing the contact function that links economic activities to contacts, the SIRD model, the dynamic economic model governing choices, and calibration. The core of our approach is a dynamic optimization model of individual behavior coupled with an SIRD model of infectious disease spread. Additional details are found in the SI.

Contact function

We model daily contacts as a function of economic activities (labor supply, measured in hours, and consumption demand, measured in dollars) creating a detailed mapping between contacts and economic activities. For example, all else equal, if a susceptible individual reduces their labor supply from 8 hours to 4 hours, they reduce their daily contacts at work from 7.5 to 3.75. Epidemiological data is central to calibrating this mapping between epidemiology and economic behaviour. Intuitively, the calibration involves calculating the mean number of disease-transmitting contacts occurring at the start of the epidemic and linking it to the number of dollars spent on consumption and hours of labor supplied before the recession begins.

We use a SIRD transmission framework to simulate SARS-CoV-2 transmission. This is supported by several studies (e.g., [72, 73]) that identify infectiousness prior to symptom onset. We consider three health types $m \in \{S, I, R\}$ for individuals, corresponding to epidemiological compartments of susceptible (S), infectious (I), and recovered (R). Individuals of health type m engage in various economic activities A_i^m , with i denoting the activities modelled. One of the A_i^m is assumed to represent unavoidable other non-economic activities, such as sleeping and commuting, which occur during the hours of the day not used for economic activities (see SI). Disease dynamics are driven by contacts between susceptible and infectious types, where the number of susceptible-infectious contacts per person is given by the following linear equation:

$$\mathcal{C}^{SI}(\mathbf{A}) = \sum_i \rho_i A_i^S A_i^I \quad (1)$$

While similar in several respects to prior epi-econ models [15, 16, 69], a methodological contribution is that ρ_i converts hours worked and dollars spent into contacts. For example, ρ_c has units of contacts per squared dollar spent at consumption activities, while ρ_l has units of contacts per squared hour worked.

We also consider robustness to different functional forms in figure 6F & G as a reduced-form way to consider multiple consumption and labor activities with heterogeneous contact rates. Formally:

$$\mathcal{C}^{SI}(\mathbf{A}) = \sum_i \rho_i (A_i^S A_i^I)^\alpha, \quad (2)$$

where $\alpha > 1$ (convex) corresponds to a contact function where higher-contact activities are easiest to reduce or individuals with more contacts are easier to isolate. $\alpha < 1$ (concave) corresponds to a contact function where higher-contact activities are hardest to reduce or individuals with fewer contacts are easier to isolate. The baseline case ($\alpha = 1$) implies all consumption or labor activities and individuals have identical contact rates (See SI section 2.3.2 for further discussion and intuition).

Calibrating contacts

To calibrate the contact function, we use U.S.-specific age and location contact matrices generated in [6], which provide projected age-specific contact rates at different locations in 2017 (shown in SI section 2.3.1). We group these location-specific contact matrices into matrices for contacts during consumption, labor, and unavoidable other activities. The transmission rate was calibrated to give a value of $\mathcal{R}_0 = 2.6$, reflective of estimates [74]. For this, we use the next-generation matrix [38]. The next-generation matrix describes the “next generation” of infections caused by a single infected individual; the \mathcal{R}_0 is the dominant eigenvalue of the next-generation matrix (see SI). This calculation is done at the disease-free steady state of the epidemiological dynamical system, when all the population is susceptible. Specifically, we calculate the benchmark number of contacts from each activity in the pre-epidemic equilibrium (e.g., $\rho_c c^S c^I$ for consumption from equation 1), under pre-epidemic consumption and labor supply levels. We then calculate the coefficients ρ_c, ρ_l, ρ_o (for consumption, labor, unavoidable other) using 1 such that pre-epidemic consumption and labor supply levels equal the benchmark number of contacts. To account for contacts that are not related to economic activities, the “unavoidable other” contact category is normalized to 1, so that the coefficient ρ_o is simply the number of contacts associated with unavoidable other activities. While pre-pandemic contact structures are necessary to calibrate \mathcal{R}_0 , our model allows contacts to evolve over time as a function of individual choices, which respond to disease dynamics.

The contact matrices in [6] measure only contacts between individuals in different age groups by activity, without noting which individuals are consuming and which are working. Given the lack of precise data on contacts between individuals engaging in different activities, we simplify by assuming individuals who are consuming only contact others who are consuming, and individuals who are working only contact others who are working. However, in reality individuals who are consuming also interact with individuals who are working (e.g., a bar or restaurant). Future work could collect more detailed contact data describing contacts between individuals engaging in different activities.

SIRD epidemiological model

The SIRD model is given by:

$$\begin{aligned} S_{t+1} &= S_t - \tau \mathcal{C}^{SI}(\mathbf{A}) S_t I_t, \\ I_{t+1} &= I_t + \tau \mathcal{C}^{SI}(\mathbf{A}) S_t I_t - (P^R + P^D) I_t, \\ R_{t+1} &= R_t + P^R I_t, \\ D_{t+1} &= D_t + P^D I_t. \end{aligned} \tag{3}$$

where S, I, R, D represent the fractions of the population in those compartments. Because the contact function $\mathcal{C}^{SI}(\mathbf{A})$ returns the number of contacts per person as a function of activities \mathbf{A} , then τ is a property of the pathogen that determines the infections per contact. This decomposes the classic “ β ” in epidemiological modeling into a biological component that is a function of the pathogen (τ) and a behavioral component linked to economic activity ($\mathcal{C}(\mathbf{A})$), such that $\beta = \mathcal{C}(\mathbf{A})\tau$ (e.g., [16]).

A key input into individual decision making is the probability of infection for a susceptible individual, which per the SIRD model above depends on the properties of the pathogen, contacts generated through economic activities, and the share of infectious individuals in the population:

$$P_t^I = \tau \mathcal{C}^{SI}(\mathbf{A}) I_t. \tag{4}$$

If a susceptible individual reduces their activities (and thus contacts) today, they reduce the probability they will get infected, which in turn reduces the growth of the infection. However, if they keep their economic behavior the same, they enjoy those benefits today, but take the risk of becoming infected in the future. Finally, P^R is the rate at which infectious individuals recover, and P^D is the rate at which they die. Both are assumed to be constant over time and independent of economic activities and contacts.

Our framework can be generalized to other structured compartmental models beyond mean-field (homogeneous) SIRD models. The key feature to translate is the contact function. For example, in an age-structured model the contact function would need to reflect age-specific consumption and labor supply patterns.

Choices

In order to analyze the three control strategies (voluntary isolation, blanket lockdown, targeted isolation), we solve two types of constrained optimization problems: a decentralized problem and a social planner problem. The decentralized problem reflects atomistic behavior by individuals—they aim to maximize their personal utility and make choices regarding economic activity. The decentralized problem is used to analyze the voluntary isolation and blanket lockdown strategies. Conversely, in the social planner problem, a social planner considers the utility of the population as a whole and coordinates economic activity to jointly maximize the utilities of all individuals in the population. Importantly, the social planner internalizes the full economic costs to the population associated with disease transmission. The social planner problem is used to analyze the targeted lockdown strategy.

In the decentralized problem, individuals observe the disease dynamics, know their own health state, and make consumption and labor choices in each period accounting for the risks incurred by contacts with

potentially infectious individuals. Let $\mathbf{A} = \{c_t^m, l_t^m\}$ represent the economic activities of consumption and labor chosen in period t by individuals of health type m . Individuals maximize their lifetime utility by choosing their economic activities, c_t^m and l_t^m , accounting for the effects of infection and recovery on their own welfare:

$$U_t^S = \max_{c_t^S, l_t^S} \{u(c_t^S, l_t^S) + \delta((1 - P_t^I)U_{t+1}^S + P_t^I U_{t+1}^I)\}, \quad (5)$$

$$U_t^I = \max_{c_t^I, l_t^I} \{u(c_t^I, l_t^I) + \delta((1 - P^R - P^D)U_{t+1}^I + P^R U_{t+1}^R + P^D U_{t+1}^D)\}, \quad (6)$$

$$U_t^R = \max_{c_t^R, l_t^R} \{u(c_t^R, l_t^R) + \delta U_{t+1}^R\}, \quad (7)$$

$$U_t^D = \Omega \quad \forall t. \quad (8)$$

Per-period utility $u(c_t^m, l_t^m)$ captures the contemporaneous net benefits from consumption and labor choices. In particular, susceptible individuals in period t recognize their personal risk of infection P_t^I is related to their choices regarding economic activity c_t^S, l_t^S , and if they do become infected in period $t+1$, they have some risk of death in period $t+2$. Death imposes a constant utility of Ω , calibrated to reflect the value of a statistical life (see SI 2.1.3). The daily discount factor δ reflects individuals' willingness to trade consumption today for consumption tomorrow.

Finally, individuals exchange labor (which they dislike), for consumption (which they do like) such that their budget balances in each period:

$$pc_t^m = w_t \phi^m l_t^m. \quad (9)$$

The wage rate w_t is paid to all individuals, per effective unit of labor $\phi^m l_t^m$, and is calculated from per capita GDP. The parameter ϕ^m captures labor productivity such that $\phi^S = \phi^R = 1$, while $\phi^I < 1$, reflecting the average decrease in productivity of infectious individuals (both asymptomatic and pre-symptomatic [24]—see SI 2.1.1). Following standard practice, the price of consumption p is normalized to 1. Finally, market equations that state how individuals are embedded in a broader economy are described in the SI.

The social planner problem coordinates the economic activities of the individuals described above. Instead of economic activities being individually chosen to maximize personal utility, the social planner coordinates consumption and labor choices of each type ($\mathbf{c}_t = c_t^S, c_t^I, c_t^R$, $\mathbf{l}_t = l_t^S, l_t^I, l_t^R$) to maximize the utility of the population over the planning horizon, subject to the disease dynamics 3 and budget constraints 9:

$$\max_{\mathbf{l}_t, \mathbf{c}_t} \sum_{t=0}^{\infty} \delta^t (S_t u(c_t^S, l_t^S) + I_t u(c_t^I, l_t^I) + R_t u(c_t^R, l_t^R) + D_t \Omega). \quad (10)$$

Additional structure (e.g., age compartments, job types, geography) can be incorporated here either by creating additional utility functions or by introducing type-specific constraints. For example, with age compartments, each age type would have a set of utility functions like equations 5–8. These would then be calibrated to reflect age-specific economic activity levels, structural parameters, and observed risk-averting behaviors.

Both the decentralized problem and the social planner problem are solved for optimal daily consumption and labor supply choices in response to daily state variable updates, and we normalize the total initial population size to 1 for computational convenience.

Utility calibration

Details of the utility function calibration and data sources are found in the SI. Briefly, economic activity levels and structural economic parameters are calibrated to match observed pre-epidemic variables for the US economy. We calibrate risk aversion and the utility cost of death to match the value of a statistical life. This approach ensures both the levels of economic choice variables and their responses to changes in the probability of infection are consistent with observed behaviors in other settings.

Model applications

We add information frictions and individual non-compliance to our baseline model to study how plausible magnitudes of such distortions may affect our policy conclusions. These are modelled by altering the inputs into agents' optimal choice rules (known as "policy functions" in dynamic optimization problems, not to be confused with pandemic control policies) that specify their (c^*, l^*) choice given the (S, I, R) information they have. The choice rules take the form shown in the equation below, where the only addition to the usual sub/superscripts is $[P]$ denoting the policy type $\{V, T, L\}$ for voluntary isolation, targeted isolation and blanket lockdown policies respectively:

$$c_{[P],t}^{*S} = c_{[P],t}^S(S_t, I_t, R_t) \quad (11)$$

$$l_{[P],t}^{*S} = l_{[P],t}^S(S_t, I_t, R_t) \quad (12)$$

All three types of agent choose consumption and labor consistent with these choice rules depending on what they know of the state of the world (i.e. (S_t, I_t, R_t)). These choice rules are the main output of the value function iteration process described in SI 3.1. By feeding different information into the choice rules or taking weighted averages under different policies, we can model the frictions described below as different scenarios.

Test reporting lags: Test reporting lags force agents to react to population-level infection information from x days ago. This is modelled as feeding $(S_{t-x}, I_{t-x}, R_{t-x})$ into the choice rules above when finding (c_t^*, l_t^*) . We select x to be roughly consistent with observed lags during the COVID-19 pandemic: initially 8 days at the outset of the pandemic, before falling to 5 days on day 60. The choice rules become:

$$c_{[P],t}^{*S} = c_{[P],t}^S(S_{t-x}, I_{t-x}, R_{t-x}) \quad (13)$$

$$l_{[P],t}^{*S} = l_{[P],t}^S(S_{t-x}, I_{t-x}, R_{t-x}) \quad (14)$$

Test quality: Tests for individual health status differ in quality throughout the course of a novel pandemic, starting from very low quality before becoming progressively more accurate. We assume that due to test quality q (for the specific foundation of this single-metric quality notion related to specificity and sensitivity see SI 3.3.2), individuals take a weighted average of the choice-rule-prescribed action for their true health type and a "no information" action which is averaged uniformly across the actions for each type. This is equivalent to either of the following behavioral microfoundations:

- individuals realize they do not know their type with certainty, so can do no better than using q to mix between the choice-rule-prescribed action for their test-reported type and an average across actions for each of the three types; or
- a fraction q of agents of a given type trust their test result and follow the associated choice-rule-prescribed action, while the remaining $1 - q$ fraction either do not get tested or do not trust their test and uniformly mix across actions for all health types.

We consider two types of test quality scenarios: first a "limited testing" scenario where test quality is low throughout the whole pandemic, and second a more-realistic "improving test quality" scenario where test quality linearly improves over the course of the pandemic, becoming perfect at day 75. The choice rules become:

$$c_{[P],t}^{*S} = qc_{[P],t}^{*S} + (1-q) \left(\frac{1}{3}c_{[P],t}^{*S} + \frac{1}{3}c_{[P],t}^{*I} + \frac{1}{3}c_{[P],t}^{*R} \right) \quad (15)$$

$$l_{[P],t}^{*S} = ql_{[P],t}^{*S} + (1-q) \left(\frac{1}{3}l_{[P],t}^{*S} + \frac{1}{3}l_{[P],t}^{*I} + \frac{1}{3}l_{[P],t}^{*R} \right) \quad (16)$$

We examine the robustness of our conclusions to an equilibrium model of behavior under low-quality information or limited cognitive capacity in SI 3.3.4, finding that the qualitative results regarding policy

effectiveness are unchanged.

Compliance: Some individuals may not comply with policy mandates. We model this as a share of agents \bar{c} of any type that choose the decentralized (i.e. voluntary isolation) action rather than complying with the targeted isolation or blanket lockdown mandates. We consider two types of scenarios, “low compliance” with 10% compliance and “partial compliance” with 75% compliance. The choice rules become:

$$c_{[P],t}^{*S} = \bar{c} * c_{[P],t}^{*S} + (1 - \bar{c}) * c_{[D],t}^{*S} \quad (17)$$

$$l_{[P],t}^{*S} = \bar{c} * l_{[P],t}^{*S} + (1 - \bar{c}) * l_{[D],t}^{*S} \quad (18)$$

References

- [1] E. Dong, H. Du, and L. Gardner. An interactive web-based dashboard to track covid-19 in real time. *Lancet Inf Dis.*, 5:533–534, 2020.
- [2] Bureau of Economic Analysis. Gross domestic product, 2nd quarter 2020 (advance estimate) and annual update. Quarterly report, Department of Commerce, 2020.
- [3] William Ogilvy Kermack and Anderson G McKendrick. A contribution to the mathematical theory of epidemics. *Proceedings of the royal society of london*, 115(772):700–721, 1927.
- [4] Christophe Fraser, Steven Riley, Roy M Anderson, and Neil M Ferguson. Factors that make an infectious disease outbreak controllable. *Proceedings of the National Academy of Sciences*, 101(16):6146–6151, 2004.
- [5] Carlos Castillo-Chavez, Derdei Bichara, and Benjamin R Morin. Perspectives on the role of mobility, behavior, and time scales in the spread of diseases. *Proceedings of the National Academy of Sciences*, 113(51):14582–14588, 2016.
- [6] Kiesha Prem, Alex Cook, and Mark Jit. Projecting social contact matrices in 152 countries using contact surveys and demographic data. *PLOS Computational Biology*, 13(9), 2017.
- [7] Kiesha Prem, Yang Liu, Timothy W Russell, Adam J Kucharski, Rosalind M Eggo, Nicholas Davies, Stefan Flasche, Samuel Clifford, Carl AB Pearson, James D Munday, et al. The effect of control strategies to reduce social mixing on outcomes of the covid-19 epidemic in wuhan, china: a modelling study. *The Lancet Public Health*, 2020.
- [8] Robert Verity, Lucy C Okell, Ilaria Dorigatti, Peter Winskill, Charles Whittaker, Natsuko Imai, Gina Cuomo-Dannenburg, Hayley Thompson, Patrick GT Walker, Han Fu, et al. Estimates of the severity of coronavirus disease 2019: a model-based analysis. *The Lancet infectious diseases*, 2020.
- [9] Benjamin M Althouse, Edward A Wenger, Joel C Miller, Samuel V Scarpino, Antoine Allard, Laurent Hébert-Dufresne, and Hao Hu. Stochasticity and heterogeneity in the transmission dynamics of sars-cov-2. *arXiv preprint arXiv:2005.13689*, 2020.
- [10] A. Aleta, Martín-Corral, A D., Pastore y Piontti, and Y. Moreno. Modelling the impact of testing, contact tracing and household quarantine on second waves of covid-19. *Nature Hum Behav*, 4:964–971, 2020.
- [11] Quan-Hui Liu, Ana I. Bento, Kexin Yang, Hang Zhang, Xiaohan Yang, Stefano Merler, Alessandro Vespignani, Jiancheng Lv, Hongjie Yu, Wei Zhang, Tao Zhou, and Marco Ajelli. The covid-19 outbreak in sichuan, china: Epidemiology and impact of interventions. *PLOS Computational Biology*, 16(12):1–14, 12 2020.
- [12] Ruiyun Li, Sen Pei, Bin Chen, Yimeng Song, Tao Zhang, Wan Yang, and Jeffrey Shaman. Substantial undocumented infection facilitates the rapid dissemination of novel coronavirus (sars-cov-2). *Science*, 368(6490):489–493, 2020.
- [13] Pierre-Yves Geoffard and Tomas Philipson. Rational epidemics and their public control. *International economic review*, pages 603–624, 1996.
- [14] Michael Kremer. Integrating behavioral choice into epidemiological models of aids. *The Quarterly Journal of Economics*, 111(2):549–573, 1996.
- [15] Eli P Fenichel, Carlos Castillo-Chavez, M Graziano Coddia, Gerardo Chowell, Paula A Gonzalez Parra, Graham J Hickling, Garth Holloway, Richard Horan, Benjamin Morin, Charles Perrings, et al. Adaptive human behavior in epidemiological models. *Proceedings of the National Academy of Sciences*, 108(15):6306–6311, 2011.

- [16] Eli P Fenichel. Economic considerations for social distancing and behavioral based policies during an epidemic. *Journal of health economics*, 32(2):440–451, 2013.
- [17] Scott Barrett. Economic considerations for the eradication endgame. *Philosophical Transactions of the Royal Society B: Biological Sciences*, 368(1623):20120149, 2013.
- [18] Charles Perrings, Carlos Castillo-Chavez, Gerardo Chowell, Peter Daszak, Eli P Fenichel, David Finnoff, Richard D Horan, A Marm Kilpatrick, Ann P Kinzig, Nicolai V Kuminoff, et al. Merging economics and epidemiology to improve the prediction and management of infectious disease. *EcoHealth*, 11(4):464–475, 2014.
- [19] Jude Bayham and Eli P Fenichel. Impact of school closures for covid-19 on the us health-care workforce and net mortality: a modelling study. *The Lancet Public Health*, 2020.
- [20] Jeremy Greenwood, Philipp Kircher, Cezar Santos, and Michèle Tertilt. An equilibrium model of the african hiv/aids epidemic. *Econometrica*, 87(4):1081–1113, 2019.
- [21] Linda Thunström, Madison Ashworth, Jason F Shogren, Stephen Newbold, and David Finnoff. Testing for covid-19: Willful ignorance or selfless behavior? *Behavioural Public Policy*, pages 1–26, 2020.
- [22] Linda Thunström, Stephen C Newbold, David Finnoff, Madison Ashworth, and Jason F Shogren. The benefits and costs of using social distancing to flatten the curve for covid-19. *Journal of Benefit-Cost Analysis*, pages 1–27, 2020.
- [23] J Lewnard and NC Lo. Scientific and ethical basis for social-distancing interventions against covid-19. *The Lancet Infectious Diseases*, 20(64):631–633, 2020.
- [24] Martin S Eichenbaum, Sergio Rebelo, and Mathias Trabandt. The macroeconomics of epidemics. Working Paper 26882, National Bureau of Economic Research, 2020.
- [25] Daron Acemoglu, Victor Chernozhukov, Iván Werning, and Michael D Whinston. A multi-risk sir model with optimally targeted lockdown. Working Paper 27102, National Bureau of Economic Research, 2020.
- [26] Miguel Faria-e Castro. Fiscal policy during a pandemic. FRB St. Louis Working Paper 2020-006, 2020.
- [27] David M Cutler and Lawrence H Summers. The covid-19 pandemic and the \$16 trillion virus. *Jama*, 324(15):1495–1496, 2020.
- [28] Raj Chetty, J Friedman, Nathaniel Hendren, and Michael Stepner. The economic consequences of $r = 1$: Towards a workable behavioural epidemiological model of pandemics. Working Paper 27431, National Bureau of Economic Research, June 2020.
- [29] Sumedha Gupta, Laura Montenovo, Thuy D Nguyen, Felipe Lozano Rojas, Ian M Schmutte, Kosali I Simon, Bruce A Weinberg, and Coady Wing. Effects of social distancing policy on labor market outcomes. Working Paper 27280, National Bureau of Economic Research, 2020.
- [30] Thuy D Nguyen, Sumedha Gupta, Martin Andersen, Ana Bento, Kosali I Simon, and Coady Wing. Impacts of state reopening policy on human mobility. Working Paper 27235, National Bureau of Economic Research, 2020.
- [31] CG Grijalva, MA Rolfs, and Zhu Y. Transmission of SARS-COV-2 Infections in Households — Tennessee and Wisconsin, April–September 2020. *MMWR Morb Mortal Wkly Rep*, 69(11):1631–1634, 03 2020.
- [32] Nancy Stokey, Robert Lucas, and Edward Prescott. Introduction. In *Recursive methods in Economic Dynamics*, pages 3–7. Harvard University Press, 1989.

- [33] Richard Bellman. Dynamic programming. *Science*, 153(3731):34–37, 1966.
- [34] Joshua Graff Zivin and Nicholas Sanders. The spread of covid-19 shows the importance of policy coordination. *Proceedings of the National Academy of Sciences*, 117(52):32842–32844, 2020.
- [35] Joël Mossong, Niel Hens, Mark Jit, Philippe Beutels, Kari Auranen, Rafael Mikolajczyk, Marco Massari, Stefania Salmaso, Gianpaolo Scalia Tomba, Jacco Wallinga, Janneke Heijne, Małgorzata Sadkowska-Todys, Magdalena Rosinska, and W. John Edmunds. Social contacts and mixing patterns relevant to the spread of infectious diseases. *PLOS Medicine*, 5(3):1–1, 03 2008.
- [36] A.I. Bento and P. Rohani. Forecasting epidemiological consequences of maternal immunization. *Clinical Infectious Diseases*, 64:1298, 2016.
- [37] Oyungerel Byambasuren, Magnolia Cardona, Katy Bell, Justin Clark, Mary-Louise McLaws, and Paul Glasziou. Estimating the extent of asymptomatic covid-19 and its potential for community transmission: systematic review and meta-analysis. *Official Journal of the Association of Medical Microbiology and Infectious Disease Canada*, 5(4):223–234, 2020.
- [38] O Diekmann, JAP Heesterbeek, and MG Roberts. The construction of next-generation matrices for compartmental epidemic models. *Journal of the Royal Society, Interface*, 7(47):873–885, 2010.
- [39] CNN. These states have implemented stay-at-home orders. here's what that means for you. <https://www.cnn.com/2020/03/23/us/coronavirus-which-states-stay-at-home-order-trnd/index.html>, 2020.
- [40] Danielle Pedi Sharon Abramowitz Simone Carter Mohamed F. Jalloh Sebastian Funk Nina Gobat Tamara Giles-Vernick Gerardo Chowell João Rangel de Almeida Rania Elessawi Samuel V. Scarpino Ross A. Hammond Sylvie Briand Joshua M. Epstein Laurent Hébert-Dufresne Benjamin M. Althouse Jamie Bedson, Laura A. Skrip. A review and agenda for integrated disease models including social and behavioural factors. *Nature Human Behaviour*, June 2021.
- [41] Maryam Farboodi, Gregor Jarosch, and Robert Shimer. Internal and external effects of social distancing in a pandemic. Working Paper 27059, National Bureau of Economic Research, April 2020.
- [42] Joshua S Gans. The economic consequences of $r = 1$: Towards a workable behavioural epidemiological model of pandemics. Working Paper 27632, National Bureau of Economic Research, July 2020.
- [43] Rahul Deb, Mallesh Pai, Akhil Vohra, and Rakesh Vohra. Testing alone is insufficient. SSRN Working Paper 3593974, 2020.
- [44] Congressional Budget Office. Monthly budget review for november 2020. Monthly report, December.
- [45] Pedro Brinca, Joao B Duarte, and Miguel Faria-e Castro. Measuring labor supply and demand shocks during covid-19. Technical report, Technical report, Federal Reserve Bank of St. Louis, St. Louis, MO, USA, 2020.
- [46] H. Scott Gordon. The economic theory of a common-property resource: The fishery. *Journal of Political Economy*, 62, 1954.
- [47] Anthony Scott. The fishery: The objectives of sole ownership. *Journal of Political Economy*, 62, 1955.
- [48] Garrett Hardin. The tragedy of the commons. *Science*, 162(3859):1243–1248, 1968.
- [49] W. D. Nordhaus. To tax or not to tax: Alternative approaches to slowing global warming. *Review of Environmental Economics and Policy*, 1:26–44, 2007.

- [50] C. Costello, S. D. Gaines, and J. Lynham. Can catch shares prevent fisheries collapse? *Science*, 321:1678–1681, 2008.
- [51] Kent D Daniel, Robert B Litterman, and Gernot Wagner. Declining CO₂ price paths. *Proceedings of the National Academy of Sciences*, 116(42):20886–20891, 2019.
- [52] Akhil Rao, Matthew G Burgess, and Daniel Kaffine. Orbital-use fees could more than quadruple the value of the space industry. *Proceedings of the National Academy of Sciences*, 117(23):12756–12762, 2020.
- [53] Tobias S. Brett and Pejman Rohani. Transmission dynamics reveal the impracticality of covid-19 herd immunity strategies. *Proceedings of the National Academy of Sciences*, 117(41):25897–25903, 2020.
- [54] D. Mistry, M Litvinova, A Pastore y Piontti, M Chinazzi, L Fumanelli, MFC Gomes, SA Haque, QH Liu, K Mu, X Xiong, ME Halloran, IM Longini, S Merler, M Ajelli, and A Vespignani. Inferring high-resolution human mixing patterns for disease modeling. *Nat Commun*, 323, 2021.
- [55] Neeraj Sood, Paul Simon, Peggy Ebner, Daniel Eichner, Jeffrey Reynolds, Eran Bendavid, and Jay Bhattacharya. Seroprevalence of sars-cov-2-specific antibodies among adults in los angeles county, california, on april 10-11, 2020. *Jama*, 2020.
- [56] Jussi Taipale, Paul Romer, and Sten Linnarsson. Population-scale testing can suppress the spread of covid-19. *medRxiv*, 2020.
- [57] Daniel B. Larremore, Bryan Wilder, Evan Lester, Soraya Shehata, James M. Burke, James A. Hay, Milind Tambe, Michael J. Mina, and Roy Parker. Test sensitivity is secondary to frequency and turnaround time for covid-19 screening. *Science Advances*, 7(1), 2021.
- [58] Michael J. Mina and Kristian G. Andersen. Covid-19 testing: One size does not fit all. *Science*, 371(6525):126–127, 2021.
- [59] Ronald H Coase. The problem of social cost. In *Classic papers in natural resource economics*, pages 87–137. Springer, 1960.
- [60] Jean-Jacques Laffont and Jean Tirole. The dynamics of incentive contracts. *Econometrica: Journal of the Econometric Society*, pages 1153–1175, 1988.
- [61] S. Flaxman, S. Mishra, A. Gandy, and Bhatt Samir. Estimating the effects of non-pharmaceutical interventions on covid-19 in europe. *Nature*, 584:257–261, 2020.
- [62] Neil M Ferguson, Daniel Laydon, Gemma Nedjati-Gilani, Natsuko Imai, Kylie Ainslie, Marc Baguelin, Sangeeta Bhatia, Adhiratha Boonyasiri, Zulma Cucunubá, and Gina Cuomo-Dannenburg. Impact of Non-Pharmaceutical Interventions (NPIs) to Reduce COVID19 Mortality and Healthcare Demand. *Imperial College London*, 10:77482, 2020.
- [63] Benjamin Roche, Andres Garchitorena, and David Roiz. The impact of lockdown strategies targeting age groups on the burden of covid-19 in france. *Epidemics*, 33:100424, 2020.
- [64] The Associated Press. At a glance: Europe's coronavirus curfews and lockdowns. <https://abcnews.go.com/Health/wireStory/glance-europe-coronavirus-curfews-lockdowns-75248293>, 2021.
- [65] USA Today. Map of covid-19 case trends, restrictions and mobility. <https://abcnews.go.com/Health/wireStory/glance-europe-coronavirus-curfews-lockdowns-75248293>, 2021.

- [66] Yiska Weisblum, Fabian Schmidt, Fengwen Zhang, Justin DaSilva, Daniel Poston, Julio CC Lorenzi, Frauke Muecksch, Magdalena Rutkowska, Hans-Heinrich Hoffmann, Eleftherios Michailidis, Christian Gaebler, Marianna Agudelo, Alice Cho, Zijun Wang, Anna Gazumyan, Melissa Cipolla, Larry Luchsinger, Christopher D Hillyer, Marina Caskey, Davide F Robbiani, Charles M Rice, Michel C Nussenzweig, Theodora Hatzioannou, and Paul D Bieniasz. Escape from neutralizing antibodies by sars-cov-2 spike protein variants. *eLife*, 9:e61312, oct 2020.
- [67] J. O. Lloyd-Smith, S. J. Schreiber, P. E. Kopp, and W. M. Getz. Superspreadering and the effect of individual variation on disease emergence. *Nature*, 438(7066):355–359, 2005.
- [68] Benjamin Rader, Samuel V. Scarpino, Anjalika Nande, Alison L. Hill, Ben Adlam, Robert C. Reiner, David M. Pigott, Bernardo Gutierrez, Alexander E. Zarebski, Munik Shrestha, John S. Brownstein, Marcia C. Castro, Christopher Dye, Huaiyu Tian, Oliver G. Pybus, and Moritz U. G. Kraemer. Crowding and the shape of covid-19 epidemics. *Nature Medicine*, 26(12):1829–1834, 2020.
- [69] Eli P Fenichel, Kevin Berry, Jude Bayham, and Gregg Gonsalves. A cell phone data driven time use analysis of the covid-19 epidemic. *medRxiv*, 2020.
- [70] Moritz U. G. Kraemer, Chia-Hung Yang, Bernardo Gutierrez, Chieh-Hsi Wu, Brennan Klein, David M. Pigott, , Louis du Plessis, Nuno R. Faria, Ruoran Li, William P. Hanage, John S. Brownstein, Maylis Layan, Alessandro Vespignani, Huaiyu Tian, Christopher Dye, Oliver G. Pybus, and Samuel V. Scarpino. The effect of human mobility and control measures on the covid-19 epidemic in china. *Science*, 368(6490):493–497, 2020.
- [71] Caroline O. Buckee, Satchit Balsari, Jennifer Chan, Mercè Crosas, Francesca Dominici, Urs Gasser, Yonatan H. Grad, Bryan Grenfell, M. Elizabeth Halloran, Moritz U. G. Kraemer, Marc Lipsitch, C. Jessica E. Metcalf, Lauren Ancel Meyers, T. Alex Perkins, Mauricio Santillana, Samuel V. Scarpino, Cecile Viboud, Amy Wesolowski, and Andrew Schroeder. Aggregated mobility data could help fight covid-19. *Science*, 368(6487):145–146, 2020.
- [72] Shixiong Hu, Wei Wang, Yan Wang, Maria Litvinova, Kaiwei Luo, Lingshuang Ren, Qianlai Sun, Xinghui Chen, Ge Zeng, Jing Li, Lu Liang, Zhihong Deng, Wen Zheng, Mei Li, Hao Yang, Jinxin Guo, Kai Wang, Xinhua Chen, Ziyan Liu, Han Yan, Huilin Shi, Zhiyuan Chen, Yonghong Zhou, Kaiyuan Sun, Alessandro Vespignani, Cécile Viboud, Lidong Gao, Marco Ajelli, and Hongjie Yu. Infectivity, susceptibility, and risk factors associated with sars-cov-2 transmission under intensive contact tracing in hunan, china. *medRxiv*, 2020.
- [73] X He, EHY Lau, P Wu, JW Deng, X Hao, YC Lau, JY Wong, Y Guan, X Tan, X Mo, Chen Y, B liao, Chen W, F Hu, Q Zhang, M Zhing, Y Wu, L Zhao, F Zhang, BJ Cowling, and GM Leung. Temporal dynamics in viral shedding and transmissibility of covid-19. *Nature Medicine*, 26:672–675, 2020.
- [74] S Sanche, Y Lin, C Xu, E Romero-Severson, N Hengartner, and R. Ke. High contagiousness and rapid spread of severe acute respiratory syndrome coronavirus 2. *Emerg Infect Dis.*, 7:1470–1477, 2020.

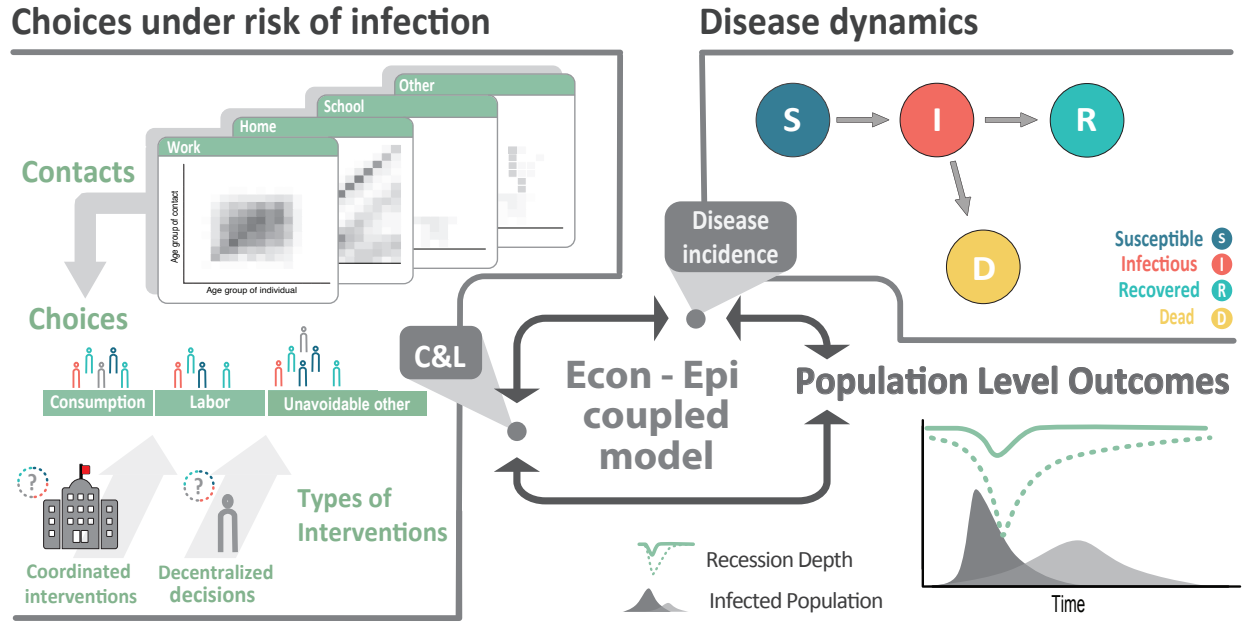


Figure 1: Coupled system schematic. Individuals make consumption and labor-leisure choices, considering the risk of infection through contacts with others. Individual choices and resulting contacts affect and are affected by the disease dynamics. Individual economic choices drive population-level outcomes such as disease prevalence and economic recessions. Under decentralized approaches, individuals optimize their behaviors based on their own preferences and health status. Under coordinated approaches, individuals' behaviors are optimized based on how they affect population-level outcomes.

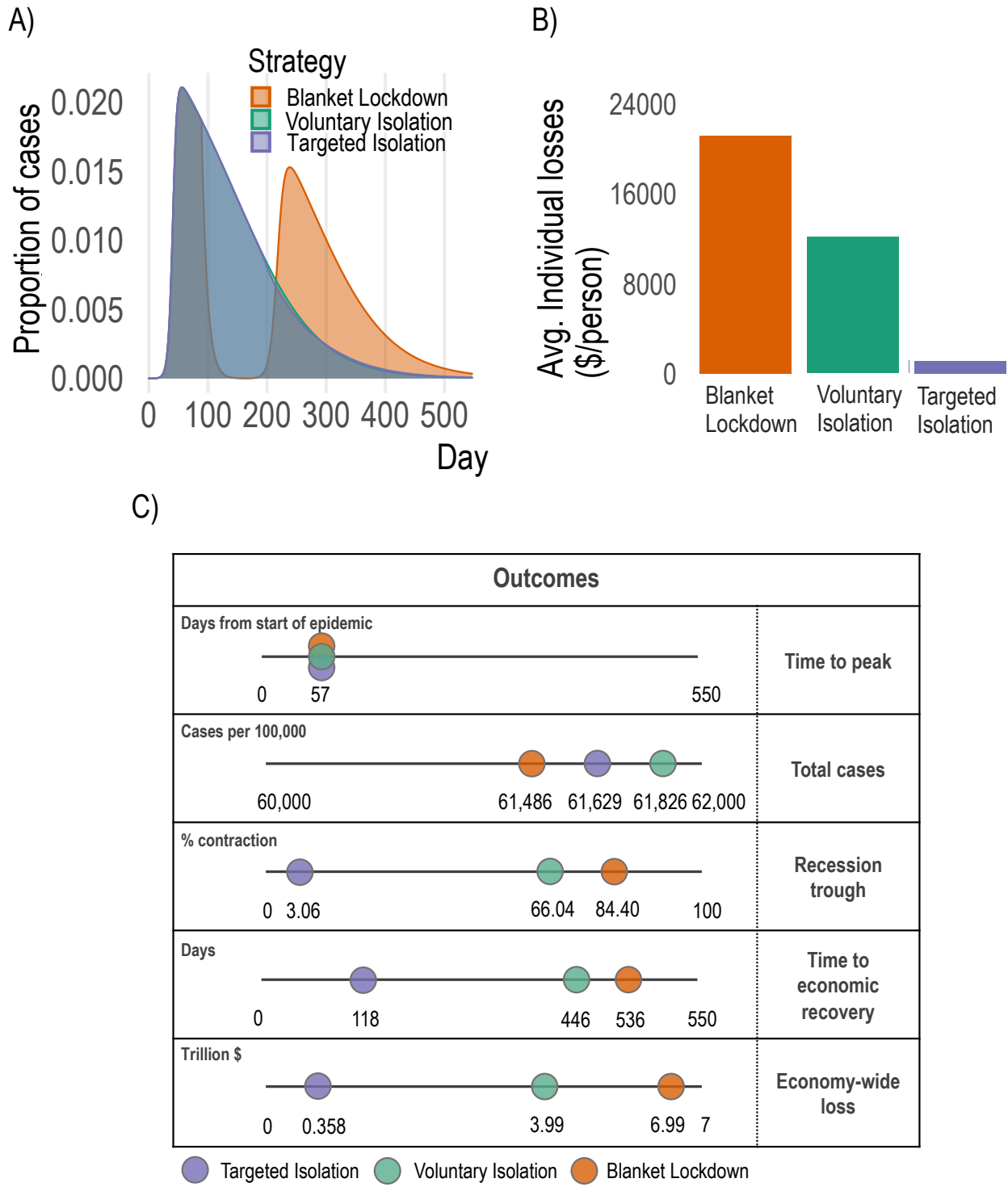


Figure 2: Disease dynamics and economic outcomes under voluntary isolation, blanket lockdown, and targeted isolation. **A:** Proportion of population infected over time under each strategy. Voluntary isolation and targeted isolation curves are almost-entirely overlapping, indicating nearly-identical disease dynamics. **B:** Individual losses incurred under each strategy (targeted isolation averts 95% of voluntary isolation individual economic losses). **C:** Key aggregate disease and economy outcomes under each strategy.

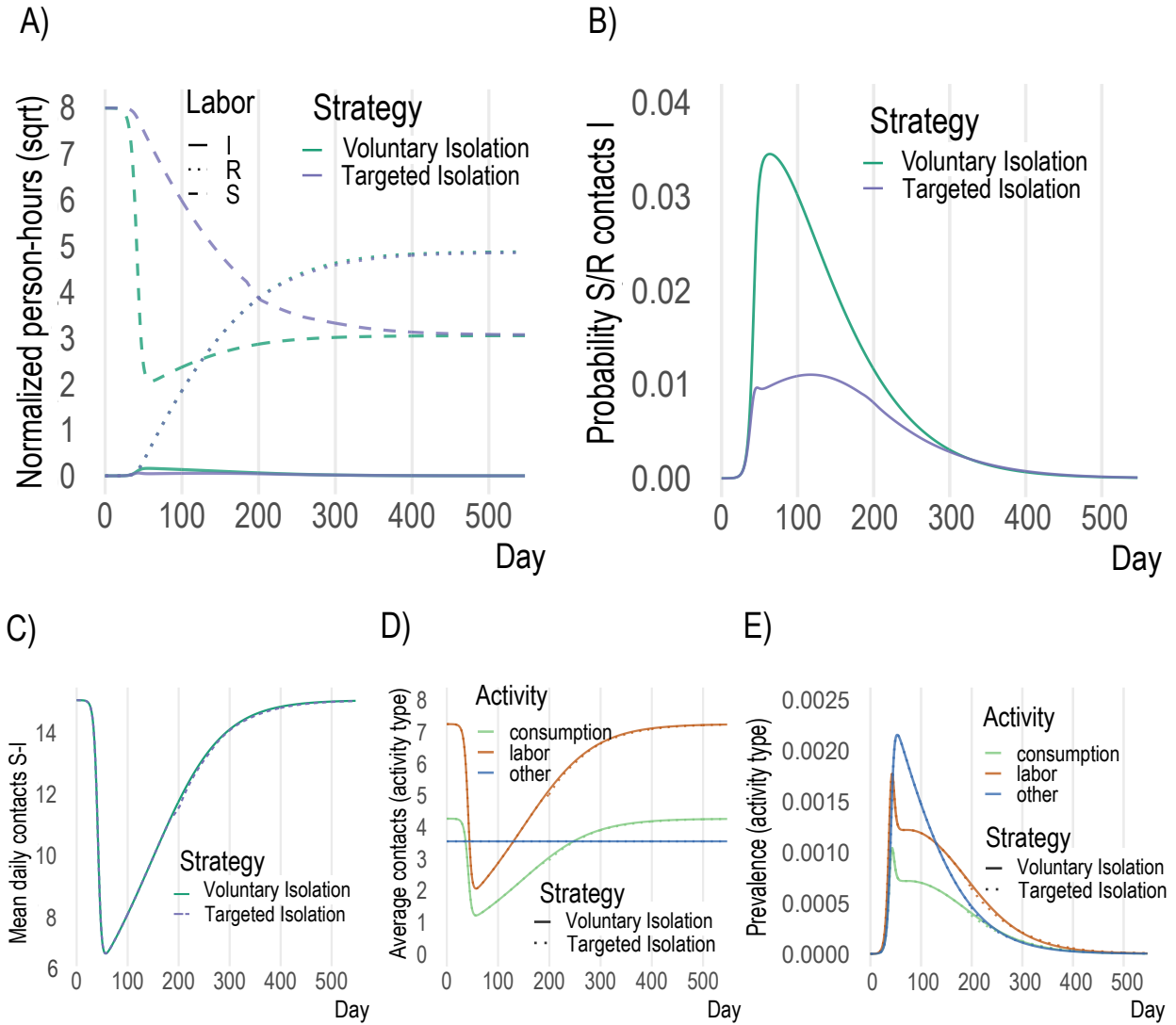


Figure 3: Key model mechanisms. **A:** in voluntary isolation, susceptible individuals withdraw from economic activity due to the presence of infectious individuals (green dashed), while under targeted isolation susceptible agents engage in much more economic activity (blue dashed). **B:** more infectious agents at activity sites under voluntary isolation leads to higher probability of infection throughout epidemic. **C,D,E:** overall contacts, contacts by activity and prevalence (% infectious) do not change meaningfully across voluntary and targeted isolation, as the same infection outcomes are achieved despite enabling far more activity by susceptible individuals with targeted isolation.

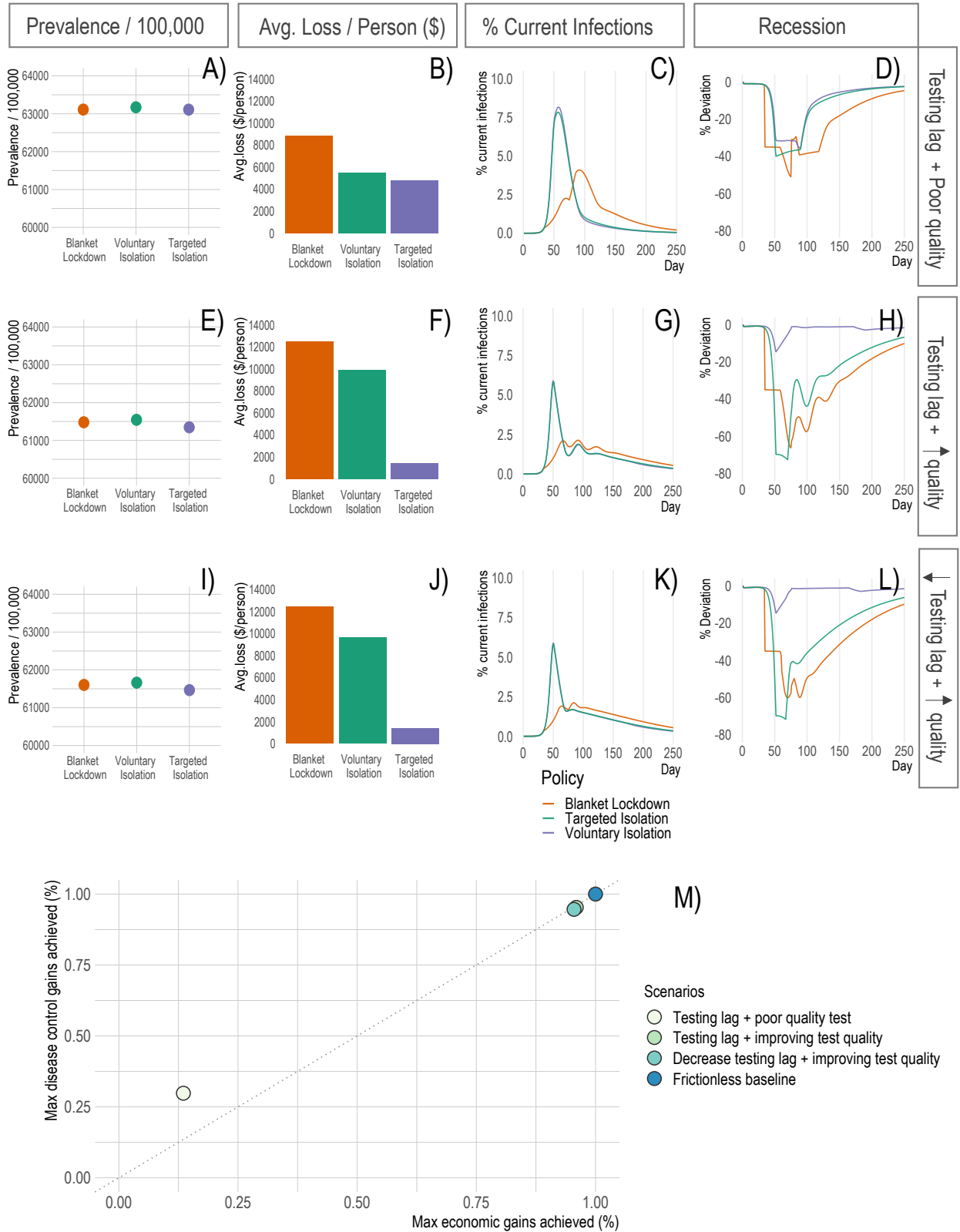


Figure 4: Model outcomes with different information frictions. Panels A-D show key model outcomes under 10% test quality and an 8-day lag between testing and reporting. Panels E-H show these outcomes when test quality linearly improves from 10% to 95% quality by day 75 under a constant 8-day test reporting lag. Panels I-L show these outcomes when test quality linearly improves as before, and the test reporting lag reduces from 8 days to 5 days at day 60. Panel M summarizes the disease-economy outcomes under these scenarios relative to the baseline in Figure 2.

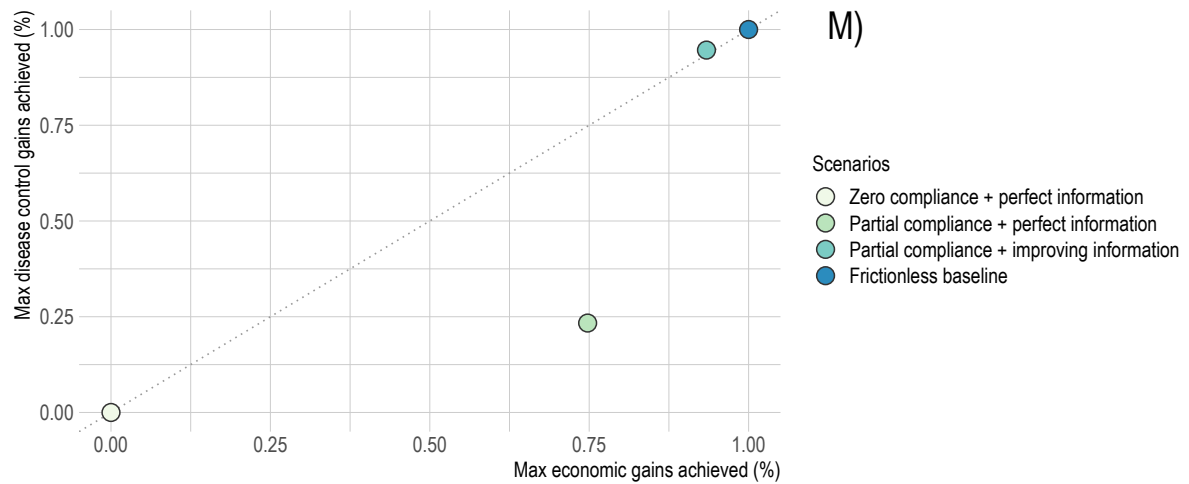
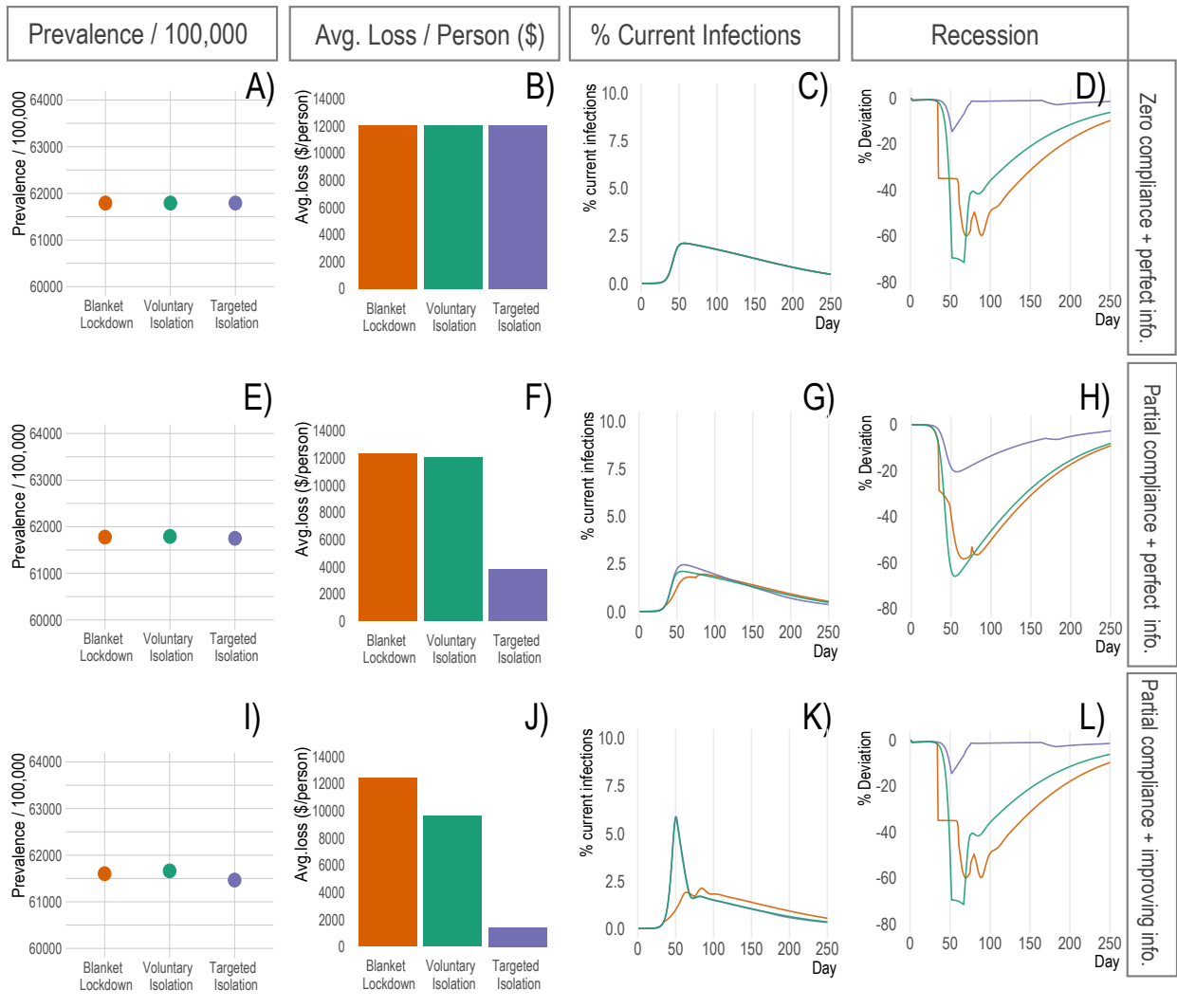


Figure 5: Model outcomes with different compliance rates. Panels A-D show key model outcomes under 0% compliance and no information frictions. Panels E-H show these outcomes under 75% compliance and no information frictions. Panels I-L show these outcomes when test quality linearly improves from 10% to 95% by day 75 and the test reporting lag reduces from 8 days to 5 days at day 60. Panel M summarizes the disease-economy outcomes relative to the baseline in Figure 2. 23

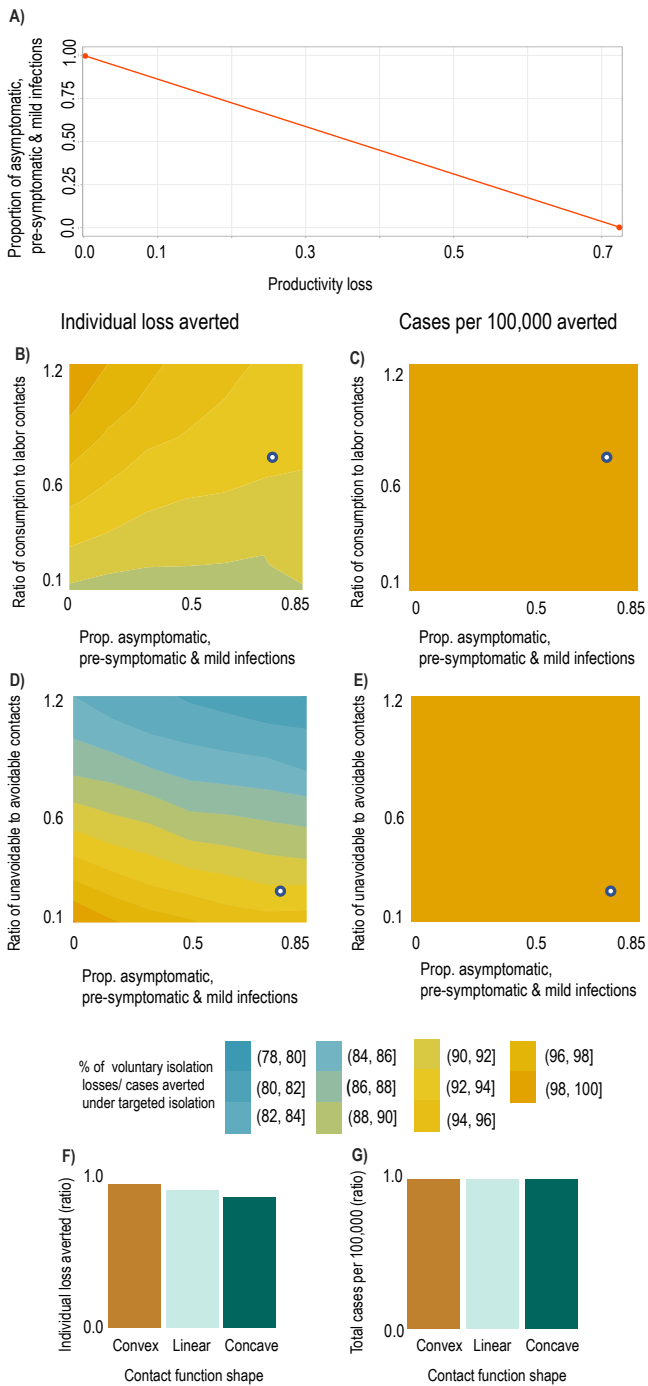


Figure 6: Result sensitivity to key model parameters. We plot ratios of outcomes under targeted vs. voluntary isolation to highlight the relative variation in outcomes under each strategy. The white dots in panels A and C show the baseline parameterization. **A:** Mapping between productivity losses and implied share of the population which is pre-symptomatic, asymptomatic, or has mild symptoms (i.e., infectious individuals able to work). A productivity loss of 0.85 implies approximately 80% of the population are pre-symptomatic, asymptomatic, or have mild symptoms. **B, C:** Ratio of individual losses averted (B) and ratio of cases per 100k averted (C) under targeted isolation vs. voluntary isolation as proportion of contacts at consumption relative to labor activities increases (a value of 1 means equal number of contacts at consumption and labor) and as the asymptomatic share increases. **D, E:** Ratio of individual losses averted (D) and ratio of cases per 100k averted (E) under targeted isolation vs. voluntary isolation as proportion of unavoidable contacts (e.g., home) relative to avoidable contacts (consumption & labor) increases (a value of 1 means an equal number of contacts at home as at consumption & labor) and as the asymptomatic share increases. **F, G:** Ratio of individual losses averted (F) and ratio of cases per 100k averted (G) under targeted isolation vs. voluntary isolation as contact functional form varies. Convex contact functions imply high-contact activities are easiest to avoid, while concave contact functions imply low-contact activities are easiest to avoid (see Materials and Methods).